SAND90-8204
Unlimited Release
Printed August 1990

SAND--90-8204

DE91 000489

A Two-Dimensional Thermomechanical Simulation of a Gas Metal Arc Welding Process

A. R. Ortega
Applied Mechanics Department
Sandia National Laboratories
Livermore, CA 94551-0969

Abstract

A low heat input gas metal arc (GMA) weld overlay process is being investigated as a possible means to repair Savannah River nuclear reactor tanks in the event cracks are detected in the reactor walls. Two-dimensional thermomechanical simulations of a GMA welding process were performed using the finite element code ABAQUS to assist in the design of the upcoming weld experiments on helium-charged specimens. The thermal model correlated well with existing test data, i.e., fusion zone depth and thermocouple data. In addition, numerical results revealed that after cool-down the final deformation of the workpiece was qualitatively similar to the shape observed experimentally. Based on these analyses, conservative recommendations were made for the workpiece dimensions, weld pass spacing, and thermomechanical boundary conditions to ensure the experiments would be as representative as possible of welding on the reactor walls.

Acknowledgements

The author gratefully acknowledges the contributions from the following: D. J. Bammann, M. L. Chiesa, R. Greif (U. C. Berkeley), G. C. Johnson (U. C. Berkeley), and L. I. Weingarten.

Contents

List of Figures

1 Introduction

In the event one of the main tanks of the Savannah River reactors develops an intergranular stress corrosion crack that either exceeds allowable size limits or leaks persistently, reactor shutdown would be required until an appropriate repair was completed. The repair of the main tanks is made exceedingly difficult because the irradiated reactor steel contains entrapped helium formed by neutron reactions with alloy constituents. Earlier experience with C reactor [1,2] and more recent experiments [3] have shown that conventional, high heat input welding techniques cannot be used with materials bearing helium at concentration levels present in production reactor vessels (1–150 appm). The observed degradation in weldability and residual properties originates from stress and temperature driven growth of cavities that are nucleated by helium gas bubbles on grain boundaries.

As an alternative to high heat input welding techniques, Westinghouse Savannah River Company has developed a relatively low heat input gas metal arc (GMA) weld overlay process [4]. Since development work is required to establish the appropriate GMA welding parameters and procedures for this application, it is important that any welding experiments on helium-charged specimens be as representative as possible of welding on the reactor walls. In particular, definitions of the proper workpiece dimensions and thermomechanical boundary conditions for the upcoming experiments are necessary to ensure that the temperature, stress, and strain distributions will be similar to those that would be anticipated during welding of the reactor walls. The issues concerning weld specimen sizing and boundary conditions are addressed numerically in this study.

Unlike the gas tungsten arc (GTA) welding process, analyses for the GMA process are limited in number because of the additional computational difficulty of modeling the transfer of molten filler metal to the workpiece. In addition, most published finite element analyses of welding processes have utilized special purpose computer codes which are not widely distributed. However, the commercially available, general purpose, finite element code ABAQUS [5] has been successfully applied to the 2D thermomechanical analysis of a GTA weld [6], and to the 3D heat transfer analysis of a GMA weld [7]. In the present study, 2D thermomechanical simulations of the GMA weld process were performed using the ABAQUS code to assist in the design of the welding experiments.

2 Computational Procedure

2.1 Modeling Approach

In the GMA welding process, a consumable electrode is fed continuously through the center of the welding nozzle. A portion of the energy supplied to the arc causes the electrode to melt. The molten filler metal is then deposited on the workpiece (as the weld overlay) forming a bond. The remainder of the arc energy is absorbed by the workpiece or is lost to the surroundings. In the GMA process analyzed here, the arc follows a sawtooth pattern resulting in a 25.4 mm (1 in) wide weld overlay. In order to simplify the modeling of this complex welding technique, local temperature variations due to the arc's oscillation were neglected.[1] That is, from the modeling viewpoint, the weld overlay is assumed to be deposited on the workpiece in a 25.4 mm wide strip.

Figure 1 is a schematic of the test set-up to be used in the welding experiments. Two weld passes are arbitrarily shown since it is likely that more than one pass will be made on a specimen prior to post-weld sectioning and examination. A weld pass initiates on the run-on tab, continues across the weld specimen, and terminates on the run-off tab.[2] The thermomechanical transients associated with arc start-up and shut-down were not treated in this study. That is, it is assumed that the thermal and mechanical problems have developed to quasi-steady state conditions.[3]

For each weld pass, it is important that the quasi-steady temperature, stress, and strain-time histories be representative of those expected for an infinitely wide plate.[4] This can be achieved experimentally by (1) providing adequate distance between adjacent weld passes, (2) providing sufficient distance between a weld pass and the edge of the plate, and (3) proper choice of the thermomechanical boundary conditions. Consider an individual weld pass (Figure 1) and take a cross-section of the specimen in the x-y plane. Specimen sizing and boundary conditions for the welding experiments can be addressed by conducting a quasi-steady 2D plane strain thermomechanical analysis on this stationary plane. Although this 2D analysis is not expected to yield a thermomechanical solution which accurately describes all of the details found in the

[1] Due to the welding process parameters, 12.7 mm (0.5 in) thick specimen, and thermal properties of the specimen, it was anticipated that temperature variations due to the arc's oscillation would be confined to the region in and near the weld overlay. Consequently, modeling this effect was not attempted since it was expected that the conclusions of this specimen sizing study would not be sensitive to local temperature variations near the weld overlay.

[2] It is assumed that the weld specimen will be made integral with the run-on/run-off tabs. Experimentally, this will be exceedingly difficult to achieve.

[3] Independent experiments [8] show that quasi-steady state conditions can be achieved.

[4] It is implicitly assumed that welding on a flat plate having infinite width is similar to welding on the 16 foot diameter reactor walls.

3D problem, particularly in the region of the weld overlay, this approximate analysis will determine the *sensitivity* of the solution to various boundary conditions and workpiece dimensions.

Sequential coupling of the thermal and stress analyses was employed in this study since it was anticipated that the heat transfer solution would only be weakly dependent on the computed displacements. This facilitates the computational procedure since the thermal analysis can be performed first, and then the mechanical analysis, in which the time-dependent temperature distributions are provided as input, can be performed.

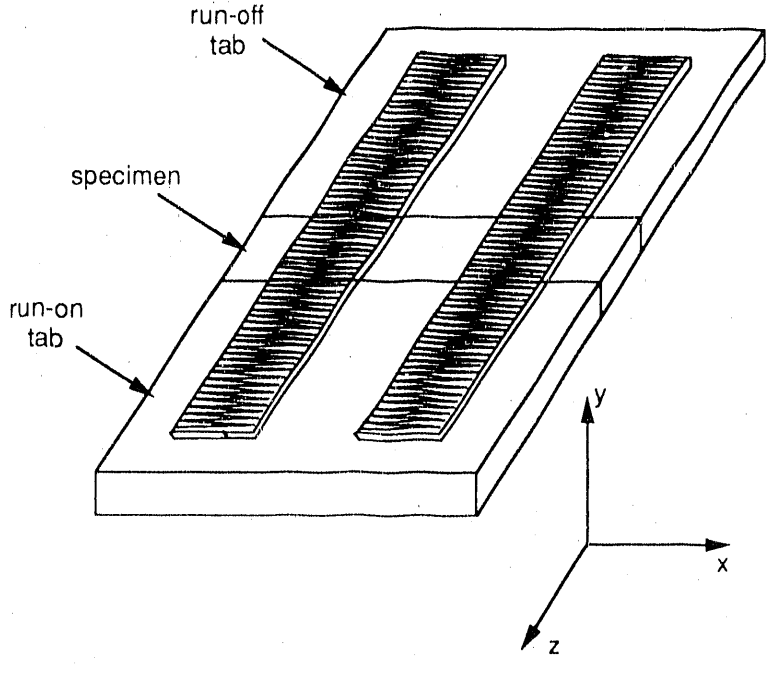

Figure 1: Schematic of the experimental set-up for GMA weld tests

2.2 Thermal Model

Various 2D finite element meshes were used in this weld specimen sizing study to model workpieces having different widths. The particular mesh shown in Figure 2 was used to correlate the thermal model with test data from instrumented GMA weld experiments conducted at WSRS[5] [8]. The computational domain depicted in Figure 2 is the half-width of the workpiece since the geometry and thermomechanical boundary conditions are symmetrical about the centerline of the weld overlay. The thickness of the plate is 12.7 mm (0.5 in), which is the nominal thickness of the Savannah River reactor tank walls. The total width of the weld overlay is 25.4 mm (1 in), and its thickness is assumed to be 1.524 mm (0.060 in).[6] Modeling the transfer of molten filler metal to the workpiece was not attempted in this analysis, rather it was assumed that the overlay was (1) a solid in intimate contact with the workpiece, and (2) included in the model prior to initiating the analysis.

The workpiece and weld overlay were assumed to be 304 stainless steel,[7] which is the same alloy used to fabricate the reactor walls. Nonlinearities associated with temperature dependent thermal conductivity and specific heat, as well as phase change,[8] were accounted for in the thermal model.[9] Nominal values for thermal losses from the top and bottom surfaces due to natural convection and radiation were also incorporated in the model. Vaporization losses are an important heat loss mechanism to model when attempting to compute accurate weld pool temperatures. However, vaporization losses were not included in the model since the goal of this analysis was to determine the *sensitivity* of the solution to boundary conditions and workpiece dimensions. In addition, heat transfer within the weld pool due to convection was neglected in this approximate analysis.

Characterization of the total heat input to the workpiece is critical to weld modeling success. In the GMA welding process, the deposition of thermal energy to the workpiece is partitioned into a heat flux which is absorbed by the workpiece, and the sensible energy contained in the weld overlay. In this study, the total heat input to the workpiece was modeled as a volumetric heat generation rate function applied to the region of the weld overlay. The thermal model was correlated with test data (i.e., fusion zone depth and quasi-steady thermocouple data) by adjusting the volumetric heat generation rate. Further details can be found in Section 3.1.

[5] Westinghouse Savannah River Site.

[6] Based on previous GMA welds, the weld overlay was modeled as being 1.524 mm (0.060 in) thick. However, the measured thickness of the weld overlay in the instrumented tests at WSRS was 0.889–1.143 mm (0.035–0.045 in) [8].

[7] The filler metal used in the experiments at WSRS [8] was 308L stainless steel.

[8] The melting range of this material was assumed to be 1673–1723 K.

[9] The thermophysical properties were obtained from Reference 9.

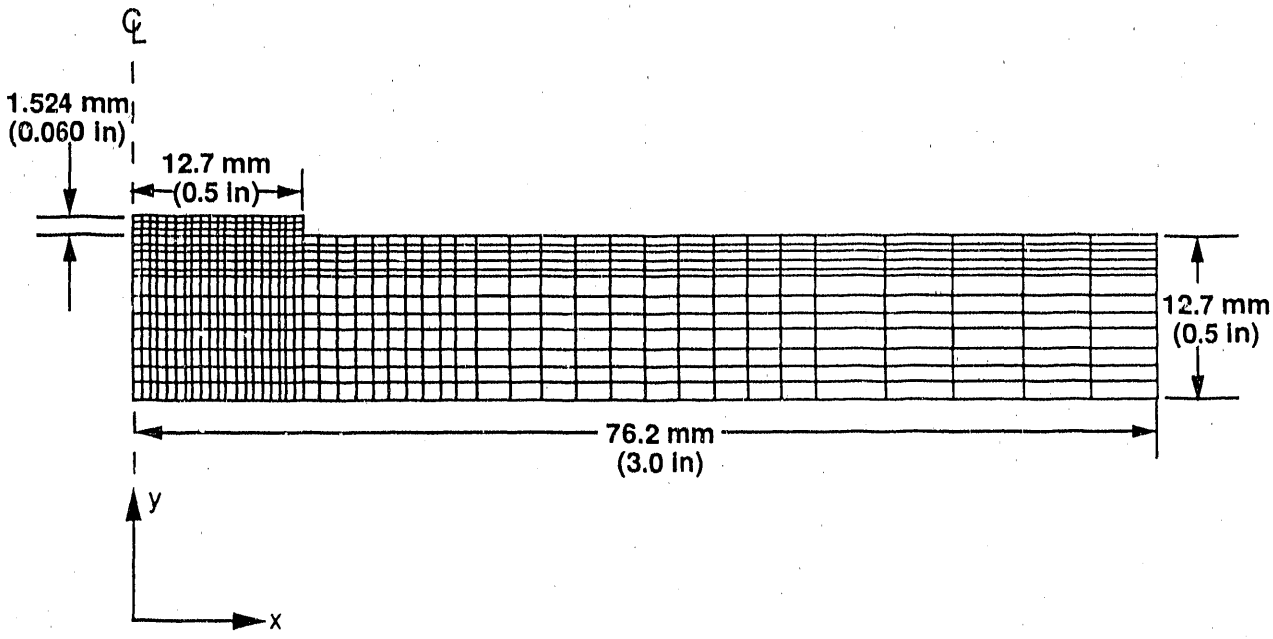

Figure 2: Finite element mesh for the 152.4 mm (6 in) wide specimen analyses

2.3 Mechanical Model

The finite element mesh for the mechanical analysis was identical to the mesh used for the heat transfer analysis (see Figure 2 for a typical mesh). Use of the same mesh for both the thermal and mechanical simulations results in the straightforward transfer of the computed nodal temperature-time histories to the mechanical model.

The plane strain assumption was imposed on the mechanical analysis. This requires the out-of-plane strains, i.e., all strain components acting in the z-direction (Figure 1), to be zero. This is the appropriate 2D approximation[10] since it is assumed that the workpiece is long in the z-direction. In addition, the coefficient of thermal expansion in the z-direction is set to zero in order to prevent computing artificially high stresses in the out-of-plane direction. This approximation is consistent with the 2D plane strain assumption.

The effect of different mechanical edge constraints on the solution was investigated in this study. The boundary conditions for the mechanical analyses are shown in Figure 3. Both fixed and free edge constraints were studied to (1) make recommendations concerning the proper boundary conditions for the weld experiments, and (2) assist in determining the infinite plate solution. That is, it is expected that the numerical results for the fixed and free edge analyses will converge to the infinite plate solution with increasing plate width.

In the prediction of stresses induced during cooling for this problem, it is important to model the temperature dependence of the elastic response, as well as model the hardening that has occurred at the onset of elastic unloading. That is, we need to know both how the material unloads and from what state the material begins the unloading process. This material behavior is accurately described in the constitutive model used in these analyses. The Bammann model [10], a strain rate and temperature dependent elastic-plastic model, introduces internal variables to describe the hardening/softening response of the material due to microstructural features such as dislocations, subgrains, and voids. The history or deformation path dependence of the material distinguishes between rate dependence of yield and rate dependence of hardening/recovery as illustrated in Figure 4 for 304L stainless steel.[11] The rate dependence of the yield stress is small at all temperatures for 304L stainless steel. Conversely, the rate dependence due to hardening/recovery mechanisms is significant at moderate to high temperatures (above 1173 K), as depicted by the increased

[10]It is recognized that strains in the z-direction are present in the 3D problem, but a 3D analysis was beyond the scope of this preliminary work.

[11]It is assumed that the difference in mechanical properties between 304 and 304L stainless steel is negligible.

rate sensitivity with increasing strain. At 293 K, the rate dependence due to hardening/recovery has a negligible effect as shown by the nearly parallel stress-strain curves.

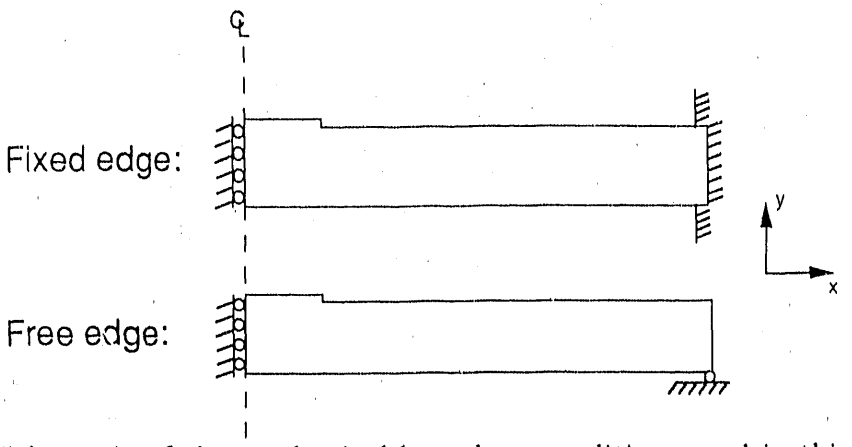

Figure 3: Schematic of the mechanical boundary conditions used in this study. For the free edge case, the node (in the finite element mesh) located on the bottom, right hand side of the plate is vertically restrained to prevent rigid body motion.

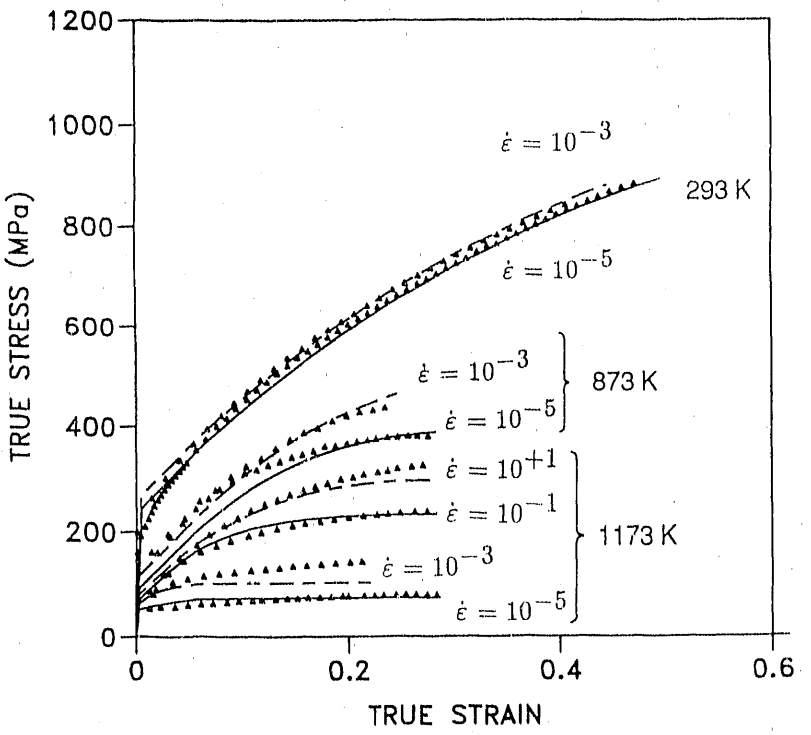

Figure 4: Comparison of the Bammann material model with tensile test data for 304L stainless steel.

2.4 Weld Pass Spacing Criteria

Since helium-charged weld specimens are not plentiful, it is prudent to make efficient use of the available material in the welding experiments. As discussed earlier, it is likely that multiple weld passes will be made on a single specimen. The weld passes will be made in a sequence such that each pass is followed by a cool-down period in which the workpiece returns to ambient conditions prior to initiating the next weld. The spacing between a weld pass and the edge of the plate, as well as spacing between adjacent passes, should be minimized subject to the constraints discussed below.

For a weld pass situated near the edge of a specimen (see Figure 1), the minimum distance between the weld and the edge can be deduced by analyzing the results of weld simulations for plates having different widths and mechanical edge constraints. That is, by comparing the results for plates of various widths, the minimum width plate which will simulate welding on an infinitely wide plate can be determined.

For adjacent weld passes, the goal is to prevent mechanical and thermal interaction between these passes. Two criteria were established in order to accomplish this objective. The first weld spacing criterion prevents the stress distribution of a weld pass from influencing the residual stress field of a previous pass. That is, this criterion requires no overlapping of the time-dependent $\sigma_{xx} = 20$ MPa (about 3 ksi) contour of a weld pass with the residual $\sigma_{xx} = 20$ MPa contour from an adjacent pass. The 20 MPa value is an arbitrary, but conservative, value for σ_{xx}, the normal stress in the x-direction. The σ_{xx} stress component was used in this criterion since σ_{xx} is the component of stress in the x-y plane that would cause the initiation of cracks oriented normal to the weld overlay. (Preliminary metallographic analysis of post-weld helium-charged specimens indicates that cracks (if detected) begin to propagate beneath the weld overlay predominately along grain boundaries which are perpendicular to the welded interface [4].)

The second spacing criterion pertaining to adjacent weld passes prevents the time-dependent thermal distribution of a weld pass from influencing the residual stress field of a previous pass. Specifically, this criterion requires no overlapping of the time-dependent 800 K isotherm of a weld pass with a residual $\sigma_{xx} = 20$ MPa contour from an adjacent pass. The 800 K temperature is a conservatively low value above which (1) thermal annealing of residual stresses is initiated, and (2) the kinetics of stress driven helium bubble growth is activated (see e.g., [11]).

3 Numerical Results

3.1 Thermal Model Verification

Instrumented GMA welding experiments were conducted at WSRS [8] to aid in the development and verification of the thermal model. In these experiments, GMA weld overlays were made on 6.35 mm (0.25 in) and 12.7 mm (0.5 in) plates to investigate the effect of plate thickness on the temperature distributions. For these thicknesses, the test results indicate that plate thickness had a significant influence on the temperature-time histories. For this reason, the thickness of the weld specimens should be 12.7 mm to ensure that future welding experiments are as representative as possible of welding on the reactor walls. The measured parameters for the welding experiment conducted on the 12.7 mm plate were: short arc metal transfer mode, current=63.5 amps, voltage drop=20.5 volts, arc oscillation speed=33.9 mm/sec (80.0 in/min), and arc forward travel speed[12]=1.16 mm/sec (2.75 in/min).

The thermal model was correlated with test data from the weld experiment described above. As discussed earlier in Section 2.2, the total heat input to the workpiece (i.e., the arc heating due to the heat flux and sensible energy contained in the weld overlay) was modeled as a volumetric heat generation rate function applied to the region of the weld overlay. This function, $\dot{Q}_V$, which is shown in Figure 5, was constructed by matching (1) the thermocouple data with computed temperature-time histories, and (2) the measured penetration depth of the fusion zone with the calculated depth. (The computed arc efficiency corresponding to Figure 5 is 73%.) High confidence thermocouple data were obtained at two locations on the weld specimen, namely, the position on the bottom surface, centerline, and the position 3.175 mm (0.125 in) below the top surface, centerline.[13] Representative quasi-steady thermocouple data at these two locations compared well with computed temperature-time histories in Figures 6 and 7.[14] Figure 8 shows the calculated fusion zone which is defined by the maximum penetration of the 1673 K isotherm. Excellent agreement was achieved between the predicted penetration depth of approximately 0.127 mm (0.005 in) and the measured value of about 0.178 mm (0.007 in) [8].

[12]This is the speed of the arc in the z-direction (see Figure 1).

[13]Although thermocouple data were obtained at other locations in the instrumented experiments, four to five thermocouples were redundantly positioned at only these two locations.

[14]The thermocouple data used in this comparison were shifted in time to account for the fact that the thermocouples were not situated in the same plane in the z-direction.

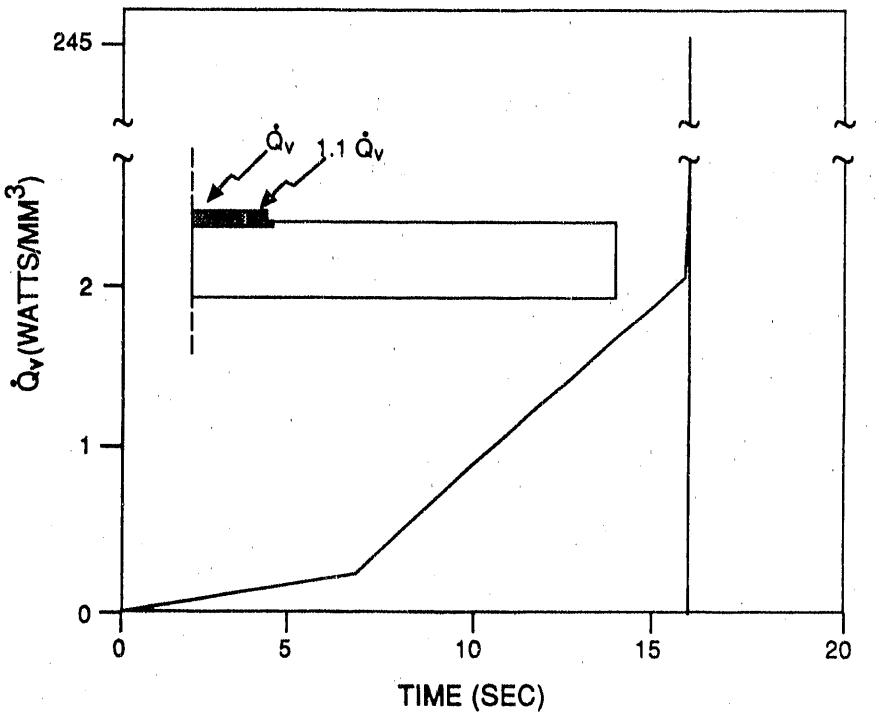

Figure 5: Volumetric heat generation rate function

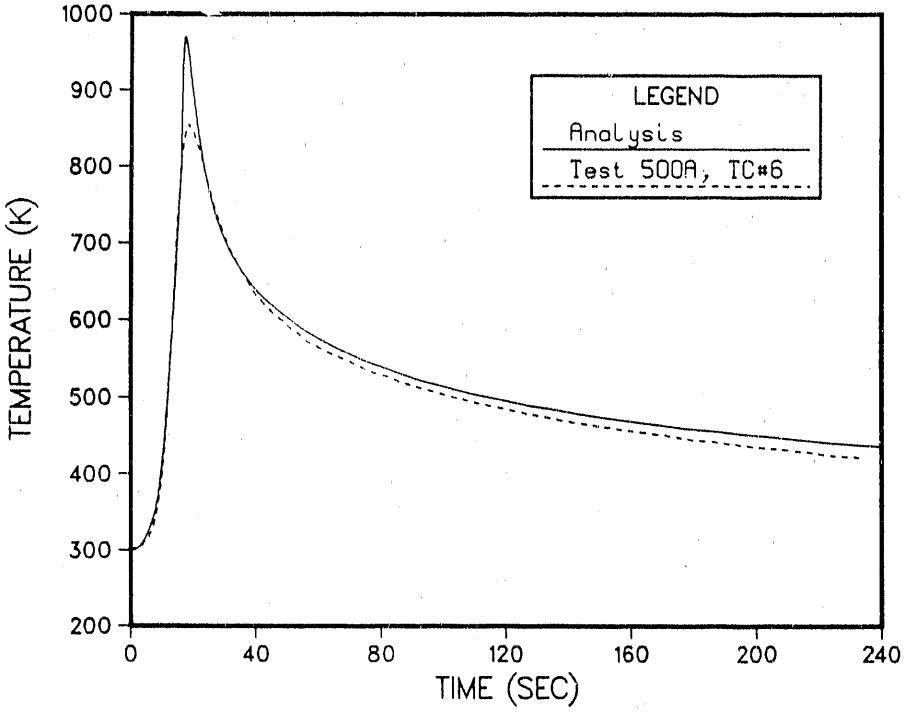

Figure 6: Comparison of numerical results with representative quasi-steady thermocouple data at the position 3.175 mm (0.125 in) from the top surface, centerline.

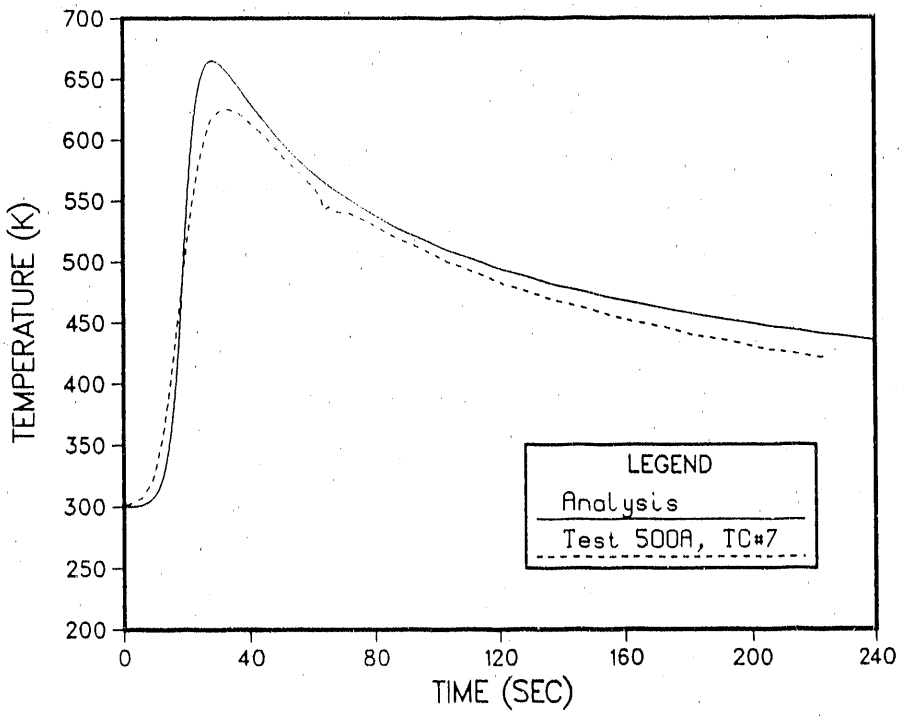

Figure 7: Comparison of numerical results with representative quasi-steady thermocouple data at the position on the bottom surface, centerline.

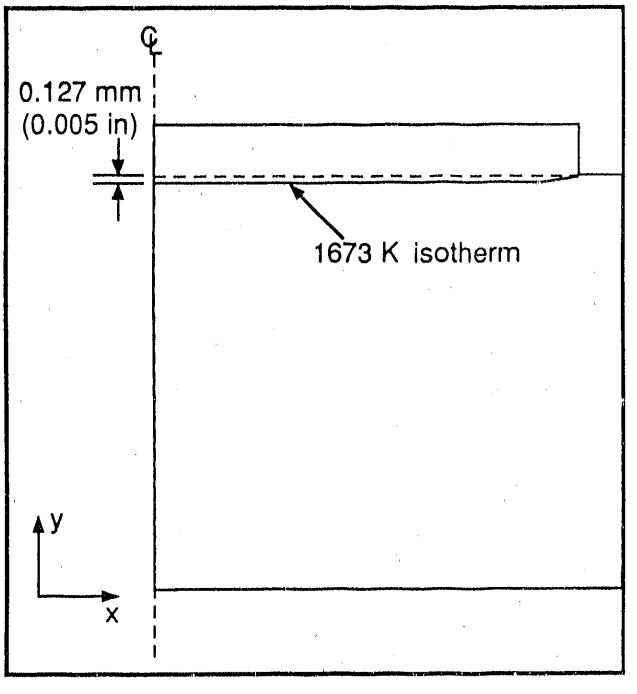

Figure 8: Calculated fusion zone. The weld overlay-workpiece interface is depicted with a dashed line.

3.2 Thermomechanical Results

Numerical weld simulations were performed for 12.7 mm (0.5 in) thick weld specimens having various widths and mechanical edge constraints. Thermomechanical results for a 152.4 mm (6 in) wide workpiece (i.e., the same width as the instrumented GMA experiments conducted at WSRS [8]) are presented first. This is followed by a discussion of the 762 mm (30 in) wide plate analyses. Finally, results are presented for a 76.2 mm (3 in) wide specimen.

152.4 mm (6 in) Wide Specimen Analyses

Numerical results pertaining to the free edge analysis are discussed first, followed by the fixed edge simulation. Thermomechanical results at 16.02 seconds after the weld simulation has begun are shown in Figure 9. This time corresponds to the maximum heat input (Figure 5) and peak weld overlay temperatures The 800 K isotherm appears in Figure 9 as the solid black contour in the temperature distribution. The noteworthy mechanical results in Figure 9 are (1) the specimen has deflected upward along the weld centerline, i.e., the plate is deformed concave down, and (2) compressive σ_{xx} stresses are generated in the weld overlay. Note that all tensile stresses below 20 MPa and all compressive stresses are illustrated in dark blue.[15]

At 17.13 seconds, the 800 K contour is at its maximum extent from the weld overlay in both the x and y directions. Figure 10 indicates that the 800 K isotherm extends nearly halfway through the plate. In addition, Figure 10 reveals that the specimen has cooled considerably leading to the development of tensile stresses in the vicinity of the weld overlay. The computed tensile stress field beneath the weld overlay[16] is consistent with the location and orientation of cracks observed metallographically [4].

At 26.38 seconds, Figure 11 shows the σ_{xx} >20 MPa stress distribution extending to its maximum lateral distance from the weld centerline, i.e., approximately 30.5 mm (1.2 in). Most of the weld overlay is now in compression, which is consistent with the displaced shape of the specimen, i.e., the plate is deformed concave up.

Figure 12 shows the numerical results at 240 seconds, after which the displacements, stresses, and strains are essentially fixed in time. Figure 12 indicates that the σ_{xx} >20 MPa residual stress distribution extends laterally about 20.3 mm (0.8 in) from the weld centerline. In addition, the final deformation of the workpiece remains concave up.

[15]This color scheme is used in Figure 9 and subsequent figures since the σ_{xx} >20 MPa distribution can be easily distinguished (see Sec. 2.4).

[16]In these analyses, the maximum principal stresses and σ_{xx} stresses were identical in the region beneath the weld overlay.

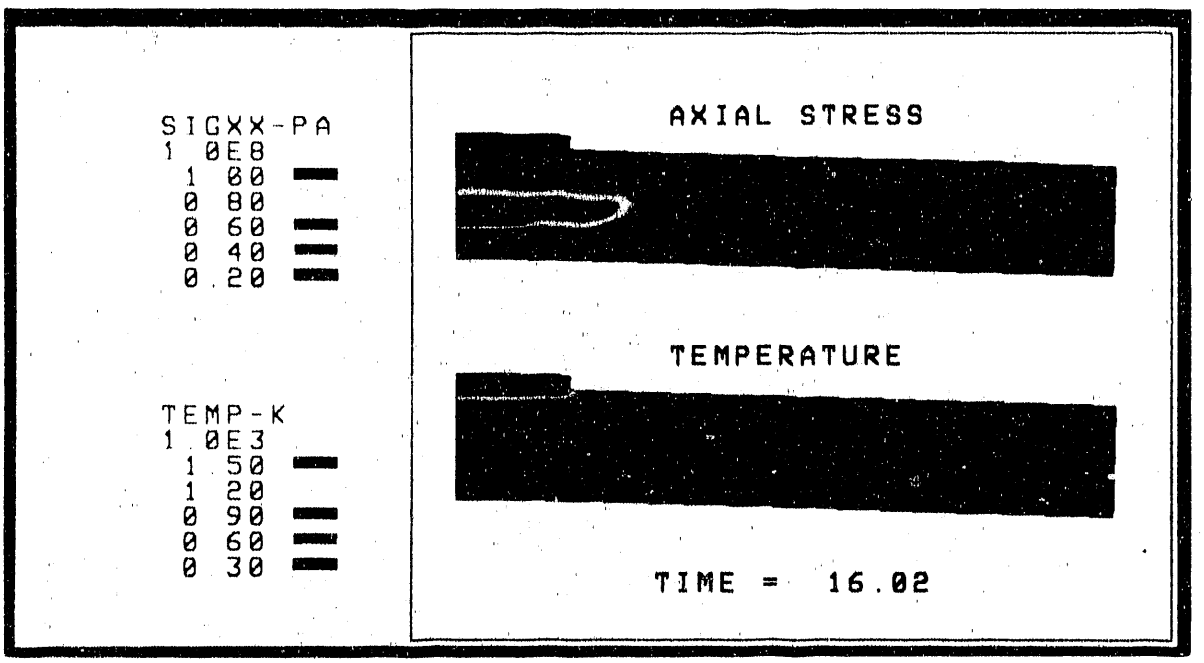

Figure 9: Thermomechanical results at 16.02 seconds for 152.4 mm (6 in) wide specimen with free edges. The displacements are magnified two times.

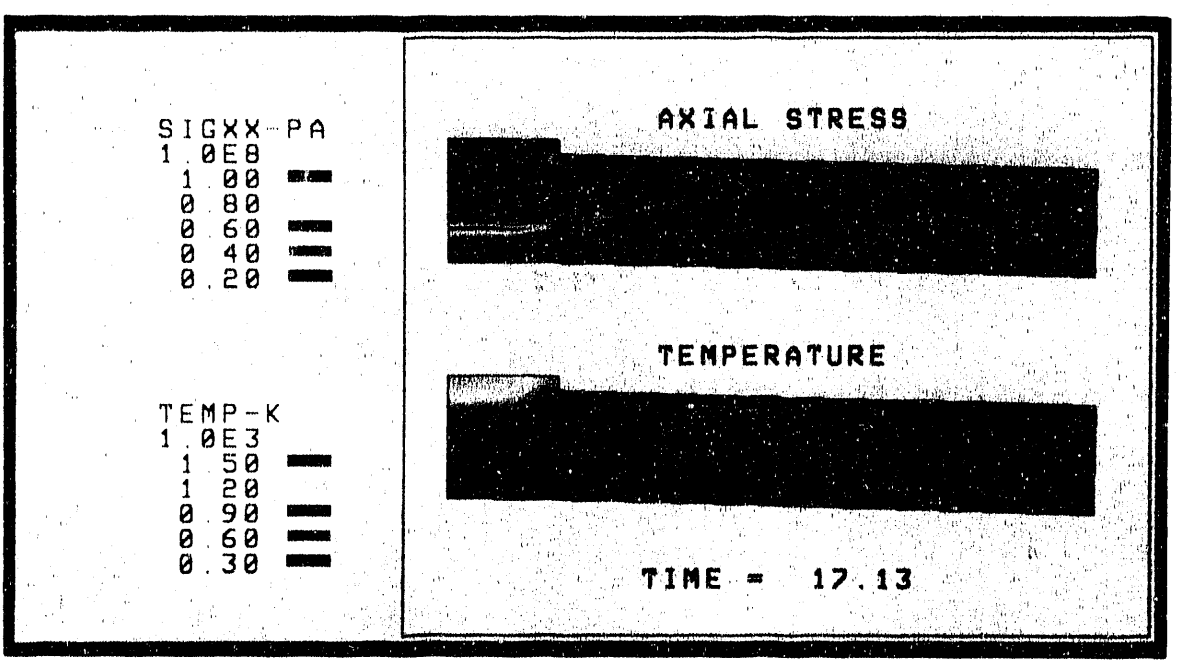

Figure 10: Thermomechanical results at 17.13 seconds for 152.4 mm (6 in) wide specimen with free edges. The displacements are magnified two times.

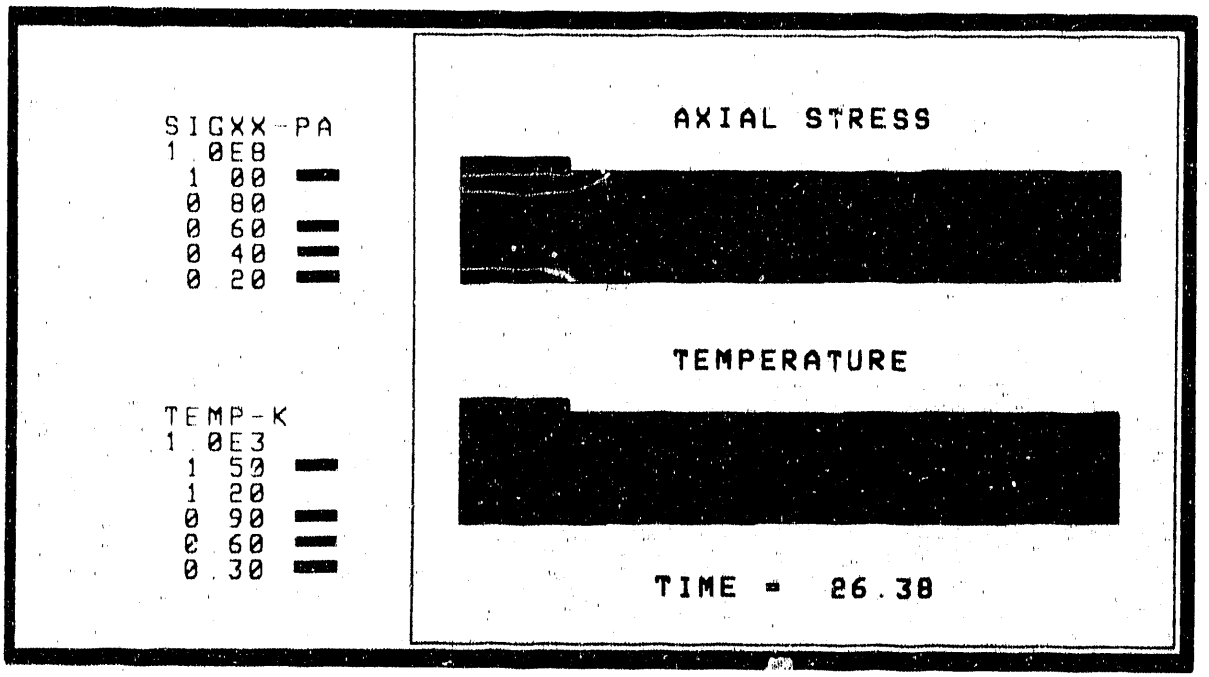

Figure 11: Thermomechanical results at 26.38 seconds for 152.4 mm (6 in) wide specimen with free edges. The displacements are magnified two times.

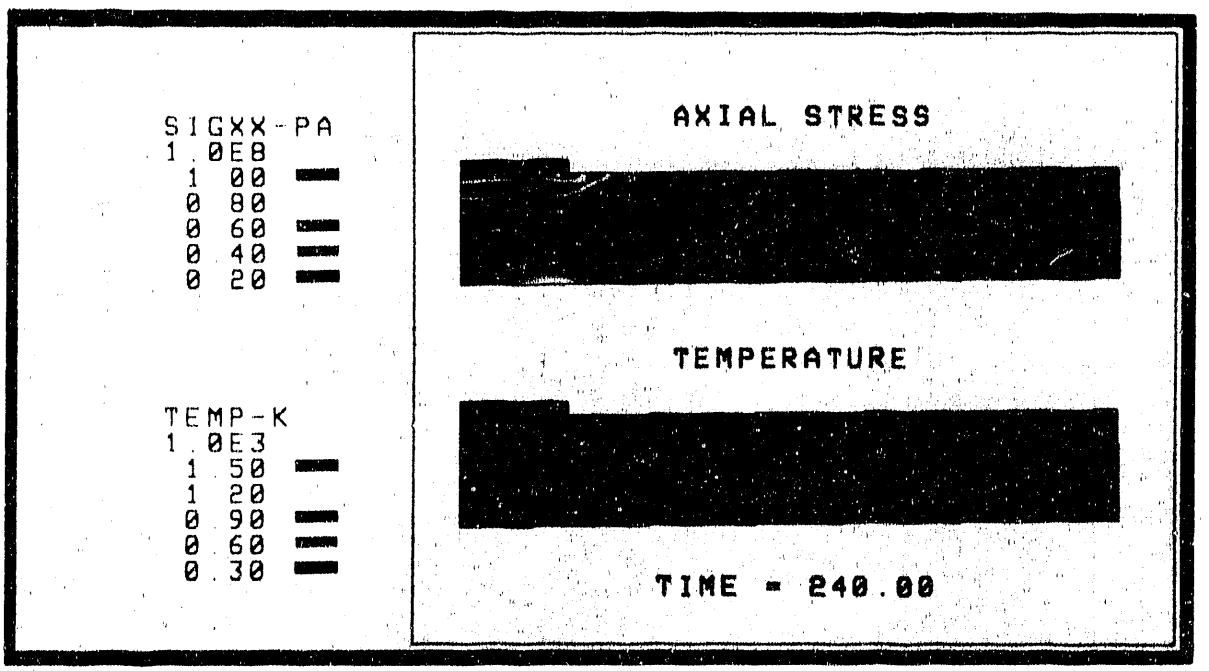

Figure 12: Thermomechanical results at 240 seconds for 152.4 mm (6 in) wide specimen with free edges. The displacements are magnified two times.

The numerical weld simulation for a specimen 152.4 mm (6 in) wide, but with the edges fixed, reveals that the edge constraint can have a significant effect on the mechanical solution. This is illustrated in Figure 13, which shows the residual σ_{xx} stress state for the fixed edge analysis. Large elastic bending stresses (approximately 200 MPa) are generated from the weld centerline to the edge of the plate. (This can be directly attributed to the fixed boundary condition at the edge of the plate.) Although the stress distributions are substantially different between the fixed and free edge analyses, the final deformation states are qualitatively similar. That is, the final shape of the specimen for both simulations is concave up. These numerical results are consistent with GMA weld experiments conducted at WSRS on plates having the same in-plane dimensions as that modeled here, i.e., 12.7 mm (0.5 in) thick and 152.4 mm (6 in) wide plate. In these experiments, the final shape of the workpiece was found to be concave up [12].

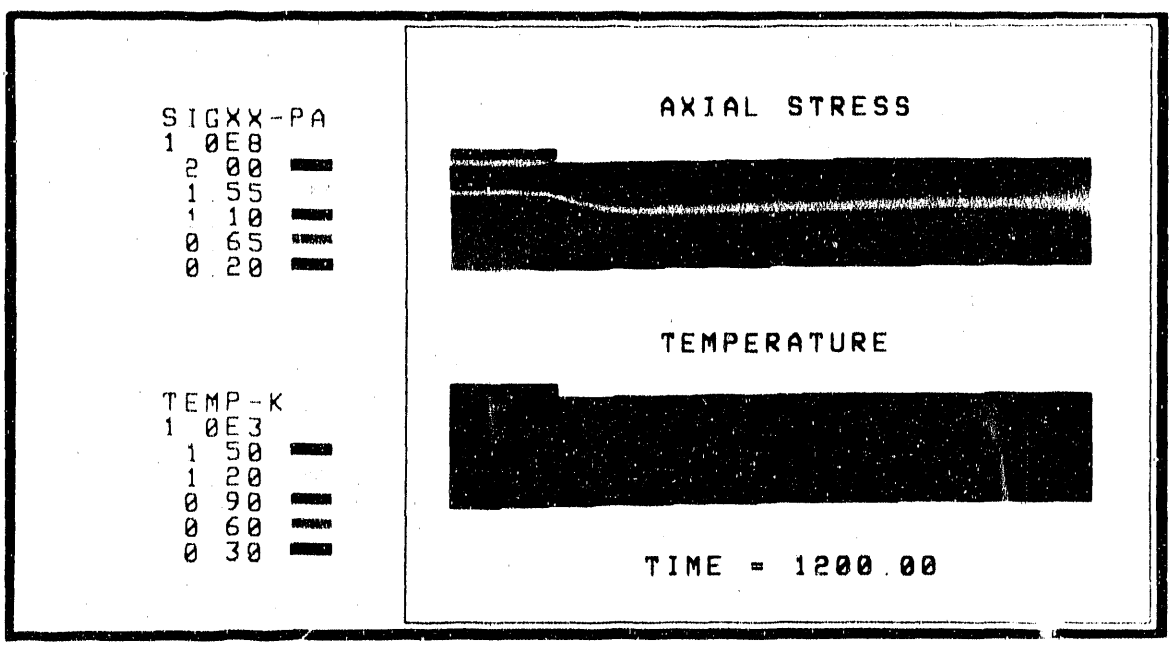

Figure 13: Thermomechanical results at 1200 seconds for 152.4 mm (6 in) wide specimen with fixed edges. The displacements are magnified two times.

762 mm (30 in) Wide Specimen Analyses

The numerical weld simulation for a specimen 762 mm wide having free edges resulted in a thermomechanical solution (in the region of the weld) which is nearly identical to the 152.4 mm (6 in) free edge analysis discussed above. That is, the results shown in Figures 9–12 for 152.4 mm with free edges are also applicable to the 762 mm wide plate with free edges. Similar stress and temperature results for both 152.4 mm and 762 mm free edge analyses suggest that these solutions are representative of the thermomechanical solution expected for an infinitely wide plate, since increasing the plate width by 5 times has only a minor effect on the solution. This is supported by the results for the 762 mm fixed edge analysis. Unlike the 152.4 mm wide specimen analyses, the character of the σ_{xx} distributions for the 762 mm fixed edge analysis is similar to that obtained for the 762 mm free edge case. In particular, the σ_{xx}-time histories for the 762 mm free and fixed analyses differed by less than 40 MPa at any point. Therefore, based on the above findings, it appears that the results for the fixed edge analyses converge to the results for the free edge simulations (Figures 9–12) with increasing plate width. In summary, the thermomechanical results presented earlier for the 152.4 mm wide plate with free edges, i.e., Figures 9–12, are similar to the numerical results expected for an infinitely wide plate.

76.2 mm (3 in) Wide Specimen Analysis

Since it was an objective of this study to minimize the distance from the centerline of a weld pass to the edge of the workpiece, specimens having widths less than 152.4 mm (6 in) were analyzed to determine the minimum width plate which would simulate welding on an infinitely wide plate. The final numerical results indicate that the stress, strain, and temperature distributions for a specimen as small as 76.2 mm wide with free edges are representative of the results obtained for the 152.4 mm plate with free edges (Figures 9–12). Therefore, the minimum width plate in which numerical results similar to the infinite plate solution can be expected is 76.2 mm.

4 Discussion

Based on the computed results, in conjunction with the weld pass spacing criteria, conservative recommendations for the spacing between adjacent weld passes, as well as spacing between a pass and the edge of the plate, can be determined. The numerical results indicate that the distance between adjacent weld passes is dictated by the spacing criterion which prevents the stress distribution (rather than the thermal distribution) of a weld pass from significantly influencing the residual stress field of a previous pass. Figures 10 and 11 reveal that the σ_{xx} >20 MPa distribution extends further from the weld overlay than the 800 K contour. In particular, Figure 12 shows that the residual σ_{xx} >20 MPa stress field is distributed approximately 20.3 mm (0.8 in) from the weld centerline, while Figure 11 indicates the maximum extent of the time-dependent σ_{xx} >20 MPa distribution is about 30.5 mm (1.2 in) from the weld centerline. Consequently, the sum of these two distances, i.e., 50.8 mm (2 in), is the minimum distance between centerlines of adjacent weld passes to prevent interaction of these passes.

Numerical stress and temperature results for a plate as small as 76.2 mm (3 in) wide are representative of the results expected for an infinitely wide plate. This implies that the minimum distance from the weld centerline to the edge of the plate should be 38.1 mm (1.5 in). In addition, the results of this study indicate that in order to obtain a mechanical response of the workpiece which is similar to that expected for an infinitely wide plate, it is critical that the specimen have free edges.

Although the results of this study have led to the above conservative recommendations for the design of the weld experiments, it is nevertheless important to exercise caution when extrapolating these results to other situations. First of all, it was not an objective of this study to obtain an accurate thermomechanical solution in and near the weld overlay, but rather to evaluate the *sensitivity* of the solution to various boundary conditions and workpiece dimensions. Therefore, care must be taken when using the computed temperature and stress distributions in the vicinity of the weld overlay since the 2D solution is not expected to be representative of the actual distributions in the 3D problem. Another caution relates to extrapolating these results to welding conditions different from those assumed in this study. If the welding procedures or weld process parameters for the experiments change significantly compared to the GMA process parameters analyzed here, the recommendations concerning weld pass spacing may no longer be conservative. For example, a substantial increase in the arc heat input would render the aforementioned recommendations non-conservative.

5 Conclusions and Recommendations

Two-dimensional thermomechanical weld simulations of the GMA welding process have been performed to assist in the design of future welding experiments. Based on these analyses, conservative recommendations were made for the workpiece dimensions, weld pass spacing, and thermomechanical boundary conditions to ensure that weld experiments on helium-bearing specimens would be representative of welding on the walls of nuclear reactor tanks at Savannah River.

The significant findings of this study, as well as recommendations for future weld experiments, are listed below.

1. Numerical results indicate that the minimum distance from the weld centerline to the edge of the workpiece should be 38.1 mm (1.5 in).

2. Results from this study show that the minimum distance between the centerlines of adjacent weld passes should be 50.8 mm (2 in). Adequate spacing between adjacent weld passes will prevent a weld pass from substantially influencing the residual stress distribution of a previous weld pass.

3. Numerical weld simulations reveal that the mechanical edge constraint has a significant influence on the stress distributions. Furthermore, a free edge boundary condition is recommended for the weld experiments.

4. Based on experimental results [8], it is clear that the thickness of the weld specimens should be identical to the reactor walls, i.e., 12.7 mm (0.5 in) thick.

5. In order to simulate welding on the reactor walls, it is recommended that the specimens be thermally isolated from the welding fixture.

6. Run-on and run-off tabs should be made integral with the weld specimen in order to prevent temperature, stress, and strain discontinuities at the specimen/tab interfaces.

Future computational efforts will be directed at developing a 3D thermomechanical capability to model any weld process which involves a weld overlay (e.g., GMA welding). The ultimate goal of this research program is to have an accurate predictive tool to evaluate various weld repair techniques.

References

[1] J. P. Maloney, "Repair of a Nuclear Reactor Vessel," E. I. DuPont de Nemours & Co., Savannah River Laboratory, DP-1199, 1969.

[2] W. R. Kanne, Jr., "Remote Reactor Repair: GTA Weld Cracking Caused by Entrapped Helium," *Welding Journal*, August 1988, pp. 33–39.

[3] H. T. Lin, S. H. Goods, M. L. Grossbeck, and B. A. Chin, *Proceedings of the 14th International Conference on the Effects of Radiation on Materials*, ASTM STP 1046, to be published.

[4] S. H. Goods and C. W. Karfs, "Helium Induced Weld Cracking in Low Heat Input GMA Weld Overlays," Sandia National Laboratories, Livermore, CA., SAND90–8404, February 1990.

[5] *ABAQUS User's Manual*, Version 4.7, Hibbitt, Karlsson, and Sorenson, Inc., Providence, R. I., 1988.

[6] L. A. Van Gulick, "Finite Element Welding Computations Using General Purpose Nonlinear Analysis Codes," *Advanced Topics in Finite Element Analysis*, J. F. Cory, Jr. and J. L. Gordon, eds., ASME, New York, N. Y., 1988, pp. 13–22.

[7] P. Tekriwal and J. Mazumder, "Finite Element Modeling of Arc Welding Processes," *Advances in Welding Science and Technology*, S. David, ed., ASM, Metals Park, OH., 1986, pp. 71–80.

[8] K. W. Mahin and J. Krafcik, "Experimental Evaluation of Gas Metal Arc Overlay Welds on the Savannah River Reactor Repair Project," Sandia National Laboratories, Livermore, CA., SAND90–8202, report in progress.

[9] *Thermophysical Properties of Selected Aerospace Materials, Part II: Thermophysical Properties of Seven Materials*, Y. S. Touloukian and C. Y. Ho, eds., CINDAS, Purdue University, Lafayette, Ind., 1977.

[10] D. J. Bammann, "Parameter Determination for a Strain Rate and Temperature Dependent Plasticity Model," Sandia National Laboratories, Livermore, CA., SAND89–8812, report in progress.

[11] K. R. Garr, D. Kramer, C. G. Rhodes, and A. G. Pard, "Helium Embrittlement of Incoloy 800," *Journal of Nuclear Materials*, Vol. 28, 1968, pp. 230-232.

[12] L. A. Bertram, K. W. Mahin, R. M. Blum, "Distorted Shapes of SRL/SNL Experimental Weld Plates," Sandia National Laboratories, Livermore, CA., memorandum, October 25, 1989.

-END-

DATE FILMED

11/05/90